Available online at www.sciencedirect.com
SCIENCE DIRECT®
Journal of Molecular Graphics and Modelling 24 (2005) 59–71
Journal of Molecular Graphics and Modelling
www.elsevier.com/locate/JMGM

Analyzing different parameters of steered molecular dynamics for small membrane interacting molecules

Alicia C. Lorenzo [a,*], Paulo M. Bisch [b,1]

[a] *Laboratório de Dinâmica Molecular, Programa de Computação Científica, PROCC, Fundação Oswaldo Cruz, FIOCRUZ, Av. Brasil, 4365 Manguinhos, 21045-900 Rio de Janeiro, Brazil*
[b] *Laboratório de Física Biológica, Instituto de Biofísica Carlos Chagas Filho, IBCCF, Universidade Federal do Rio de Janeiro, UFRJ, CCS, Bloco G, Ilha do Fundão, 21949-9000 Rio de Janeiro, Brazil*

Received 19 July 2004; received in revised form 11 May 2005; accepted 11 May 2005
Available online 5 July 2005

Abstract

The aim of this report is two-fold: First, to show the applicability of the Steered Molecular Dynamics (SMD) methodology for analyzing non-specific interactions governing the membrane affinity process of small biological molecules. Second, to point out a correlation between the system response and certain combinations of the SMD parameters (spring-elastic-constant and pulling-group). For these purposes, a simplified membrane model was used, modeled as a non-polar region limited by two polar aqueous media in a continuous dielectric representation. Polarization-induced effects at both interfaces were taken into account by the ''electrostatic images'' method. To perform SMD simulations a harmonic external force, representing a spring acting on a selected atom, forces the molecule to ''break'' its interaction with the surrounding environment by extracting it out of the membrane. With this approach, small molecules and peptides, with known affinity for the membrane environment, were studied: the zwitterionic tryptophan residue and a pentapeptide AcWLKLL. The SMD parameters, spring-elastic-constant and pulling-group, were varied and combined in order to analyze the systems responses in each case. It was observed that, the spring stiffness was crucial to reveal specific events that occur during the molecule behavior; hence, it was directly responsible for the sensitivity of this methodology. The pulling-group selected highly influenced on the reaction pathway, a fact that it was not observed with other parameters; consequently, force profiles are like the ''fingerprints'' of these induced pathways. The potential profile for the tryptophan was recovered from the SMD simulations being in good agreement with that estimated by an approximation method. With this rather simple model approach, SMD methodology has proven to be suitable for revealing the main interactions that govern the membrane affinity processes of small molecules and peptides.

Keywords: Steered molecular dynamics simulations; Non-specific interaction forces; Membrane-interacting systems; Simulation parameters

1. Introduction

Some biological molecules and peptides present great affinity for a specific inhomogeneous environment: a biological membrane. Particularly, several biologically active molecules depend on how well they are adapted to this medium in order to express their natural functions. In the adaptation process these molecules undergo several conformational changes due to a delicate balance between their intramolecular forces and their interactions with the surrounding environment. Several non-covalent forces characterize these interactions; ranging from long-range interactions like van der Waals and Coulomb forces, to short-range interactions, like hydrogen bonding and salt-bridge formation. However, the basis by which membrane contributes to the specificity of these processes at a molecular level is not known. Besides, the difficulty of sorting out the relative contributions of these various possible interactions makes hard to predict or understand the adaptation and stabilization mechanisms of these molecules in the membrane environment. These difficulties have stimulated the development of smaller peptide models of

* Corresponding author. Tel.: +55 21 2573 0234x124; fax: +55 21 2270 5141.
E-mail addresses: alicia@fiocruz.br (A.C. Lorenzo), pmbisch@biof.ufrj.br (P.M. Bisch).
[1] Tel.: +55 21 2562 6575; fax: +55 21 2280 8193.

1093-3263/$ – see front matter © 2005 Elsevier Inc. All rights reserved.
doi:10.1016/j.jmgm.2005.05.005

proteins that retain some properties of larger proteins and the regular implementation of these models for studying a particular biological process. In addition, based on an experimental technique, the Steered Molecular Dynamics (SMD) methodology was developed to provide, along the induced response pathway, detailed information in terms of conformational changes and interacting forces in a hierarchical way. This information permits the interpretation at the atomic level of particular events and characteristics of the molecular behavior, usually unavailable to experimental techniques.

The aim of this work was to test the SMD method on a different biological problem that has been studied so far with this technique: to investigate the driving forces that governs the affinity process of small membrane interacting biomolecules and peptides. For this purpose, it became necessary to compare our results to those obtained with an extensively investigated problem by SMD: the induced unbinding of ligands [1–3] in terms of the global results and features that this technique can offer. SMD has already provided useful insights into several biologically relevant questions in a variety of molecular systems [4–9]; however, we observed that the amount and type of information that can be extracted highly depend on the appropriate combination of the simulation parameters. Consequently, this study was focused on the characterization of these parameters, mainly, the spring elastic constant and the pulling-group in terms of the systems responses.

Two simple systems were selected for the analysis: the zwitterionic tryptophan amino acid, commonly studied for the spectral properties of its aromatic ring; highly sensitive to the environment, it can reflect structural characteristics of proteins when it is exposed to the solvent or buried in the protein interior. This residue becomes a good computational model because its conformational states have been extensively studied by several techniques, such as Nuclear Magnetic Resonance (NMR) [10,11], X-ray Crystallography [12] or molecular mechanics simulations for the zwitterionic state [13–15]. The other system was the pentapeptide AcTrp-Leu-Lys-Leu-Leu, initially modeled by W. Wimley and coworkers in 1996 to measure the solvation energy of a salt-bridge formed between its carboxyl terminal and its lysine side chain [16]. This was done by determining the free energy variations when the peptide was transferred from octanol to a buffer solution at different pH values. The formation of this salt-bridge, observed only in a basic octanol phase, would be the explanation of a ''hydrophobic'' behavior detected when compared with the same peptide where a glycine was considered in place of the lysine. In an acid medium, the carboxyl terminal would be protonated, hence, no salt-bridge could be formed. A Monte Carlo simulation of this peptide in vacuum was also done by W. Wimley, showing the feasibility of this salt-bridge formation [16–18]. Both systems were previously studied by means of molecular dynamics (MD) technique. Simulations were performed in water and in the membrane environment. To investigate the underlying reasons for their membrane affinity, the SMD methodology was implemented.

2. Methods

A computational package THOR [19–21] for molecular modeling and dynamics, based on the Gromos96 force field [22,23], was modified to incorporate the SMD technique.

Non-explicit medium representation, characterized by the dielectric constant ε was considered. The polar or aqueous medium was represented by $\varepsilon = 78$, as proposed by J. Israelachvilli for water at 25 °C (300 K), ($\varepsilon = 80$ was suggested for 20°) [24,25]. The non-polar or hydrophobic medium was represented by $\varepsilon = 4$, according to the dependence of the dielectric constant with the extension of the hydrocarbon lipid tails determined by S.D. Evans in an experimental work. This study shows a rapid decline of the ε from 8 to 4 when the number of carbon atoms of the lipid chain increases from 6 to 10 approximately, and a smooth variation from 4 to 2 for an increment of the carbon atoms from 10 to 22 ($\varepsilon = 2$ is assigned to the bulk). On the other hand, C. Tanford proposed a correlation between the extension L of the unsaturated lipid chains with the number of carbon atoms N as $L_{\max} \approx (0.154 + 0.1265\,\mathrm{N})$ nm, representing an extension of around 14 Å for $N = 10$, for each monolayer [26]. Accordingly, for our membrane model of 30 Å wide, an ε of 4 was chosen for the non-polar region.

In a basic membrane model the hydrophobic region is limited by the two surfaces that are in contact with the polar aqueous medium. However, this simplified approach introduces a dielectric discontinuity on both interfaces reflected as a discontinuity on the electrostatic potential. On the other hand, when a molecule is in the presence of this non-homogeneous environment, polarization charges are induced over these surfaces. This induced polarization is originated by the electronic displacements in atoms and chemical bonds and by the reorientation of the dipoles of the solvent molecules. These polarization effects were considered in our membrane model on the bases of the Electrostatic Image method [15,20,27,28]. An extra electrostatic term for the hypothetical charges, images of the molecular charges, was incorporated in the force field to solve the induced charge effect. This approach, not only improved the representation of the molecule-membrane interactions, but also solved the discontinuity problem by introducing a continuously smooth variation of the electrostatic potential energy at the interfaces [15]. This membrane characterization has already provided a good description of physicochemical and conformational properties of several studied systems [15,19–21,29–31].

To perform the SMD simulations, an additional one-dimensional elastic force (a spring representation) was incorporated to the THOR force field. This force acts on a selected atom of the molecule where one end of the spring is fixed. The other end of the spring, is displaced at constant

velocity, forcing the molecule to exit the membrane. The displacement, in X-direction, is perpendicular to the membrane interfaces. Due to action–reaction principle, the spring acts as a sensor of all interacting processes along the selected exit pathway. The elastic force is proportional to the spring elongation relative to its equilibrium position, and it is given by the expression

$$F_i = -K[x_i(t) - x(t)]$$

$$x(t) = Vt + x^0$$

Where F_i is the force experienced by the atom-i fixed to the spring due to the action of this probe, x_i (t) is the X-coordinate of the atom-i as a function of time t, and $x^0 = x_i$ $(t = 0)$ in order to have a zero extra force at initial time $t = 0$, where the spring should be relaxed. V is the constant pulling velocity.

2.1. MD and SMD simulations

All systems were initially studied by means of MD where the following steps were performed

(a) Selection of the Initial molecular conformation for MD simulations:
The aromatic ring of the zwitterionic tryptophan was modeled in a full atom representation. The six minimum energy rotamers of this amino acid (*perp*-$\chi_2(t)$, *perp*-$\chi_2(g^+)$, *perp*-$\chi_2(g^-)$, *anti*-$\chi_2(t)$, *anti*-$\chi_2(g^+)$ and *anti*-$\chi_2(g^-)$ were selected as the initial conditions for the MD simulations. For the synthetic peptide AcWLKLL, no structural conformation was available, thus a computational predicting procedure was implemented: the *Dynamic Annealing* method. This method is based on an extended MD simulation that alternates cycles of high temperature followed by a gradual cooling process. An arbitrary molecular structure is considered initially at a low temperature (∼50 K), then, it is rapidly (∼0.05 ps) heated up to 2000 K, inducing the surmounting of high potential barriers and facilitating the adoption of diverse conformational states. Thereafter, it is gradually cooled down (20 ps) up to 10 K. All conformational dihedral angles are registered after the cooling process of each cycle. The peptide structure is determined by a statistical analysis performed over thousands of these dynamic cycles.
(b) Optimization: conformations were optimized by means of the steepest-descent algorithm [32] with a convergence of 10^{-5} kcal/mol.
(c) Heating up process: MD simulations were initiated by gradually increasing the temperature every 30 steps (0.5 fs per step), from 10 K up to 300 K.
(d) Thermalization: simulations were prolonged for hundreds of nanoseconds at a constant temperature (300 K) in the presence of a thermal bath [33].

Both systems, the amino acid tryptophan and the pentapeptide AcWLKLL, were studied initially by means of MD, where steps (b), (c) and (d), mentioned above, were performed out of the membrane, in the aqueous medium. In both cases, when molecules where simulated in presence of the membrane environment, the insertion occurred spontaneously, and MD simulations were prolonged until a molecular stable structure was reached in this medium, providing the initial conformational state for the SMD simulations.

In SMD simulations, the molecule was pulled out at a constant velocity, in X-direction, perpendicular to the membrane–water interface. The two membrane interfaces, were considered as infinite planes, separated by 30 Å. All simulations were carried out in the presence of the thermal bath mentioned above. To perform a SMD simulation, three parameters should be selected: the pulling velocity V, the pulling-group (atom or group of atoms of the molecule attached to one spring end) and the elastic constant k of the spring (stiffness of the restraint). This work was focused on the analyses of the systems responses for different restraint stiffness and pulling-groups. The pulling velocity was thoroughly explored for a broad range of values in a previous work [21]. Accordingly, three SMD simulations with different spring constants: $k_1 = 0.1$, $k_2 = 0.6$ and $k_3 = 4$ kcal/mol Å^2 (7, 40 and 280 pN/Å) are presented in this report for the amino acid tryptophan. k_1 and k_2 correspond to typical experimental spring (cantilever) constants, where k_1 is usually considered as a soft spring. k_3 does not represent an experimental value, but it has been used in several SMD studies [1,2,4,6] being the stiffest spring considered in this type of simulations. All other parameters were taken the same: the pulling velocity $V = 0.015$ Å/ps (1.5 m/s) and the pulling-group was one of the oxygen atoms of the C-terminal (COO^-). A correlation between the stiffness of the applied restraint with the sensitivity of the technique is discussed for this residue. For the pentapeptide AcWLKLL, two SMD simulations are presented where different pulling-groups were considered: the N- and C-terminal of this peptide. Accordingly, the extraction pathways and the system responses for these two pulling-groups were analyzed. In accordance with the experimental model, the C-terminal was considered charged (COO^-) and the N-terminal was acetylated. A summery of general results is presented for this peptide.

3. Results and discussions

3.1. Zwitterionic tryptophan

3.1.1. MD simulations

The tryptophan amino acid was studied by means of MD simulations to obtain a statistical mapping of all conformations in three media (aqueous, hydrophobic and membrane interior). Extended simulations were performed (80–100 ns)

to guarantee stabilized structures considering that an implicit medium representation lacks of the damping effect of the molecular solvent. The first 10 ns approximately, the tryptophan fluctuated among all six minimum energy rotamers ((*perp*-$\chi_2(t)$, *perp*-$\chi_2(g^+)$, *perp*-$\chi_2(g^-)$, *anti*-$\chi_2(t)$, *anti*-$\chi_2(g^+)$ and *anti*-$\chi_2(g^-)$) independently of the initial state. A higher interconversion rate was observed between the two χ_2 rotamers compared with the three χ_1 forms (g^+, g^- and t). This behavior was also mentioned by Gordon and coworkers in a conformational study of the zwitterionic tryptophan for simulations of 1ns, with a continuous medium representation and with explicit water [14]. In addition, frequently interconversions of the χ_2 conformer *perp*-χ_2 ($\chi_2 = 100^\circ$) to $\chi_2 = 150^\circ$ were detected in our simulations (also mentioned in Gordon's work) ($\chi_2 = 150^\circ$, also corresponds to a minimum of the torsional potential energy). In our simulations, this fluctuating behavior were observed for around 10 ns and, after that, the residue adopted one of the identify conformations. At this point, the molecule was considered stabilized, where the dihedral angle fluctuations remained around $\pm 5^\circ$ for the rest of the simulation. In the membrane environment, the tryptophan residue adopted predominantly the *perp*-$\chi_2(g^-)$ conformational state when stabilized. Fig. 1a shows the zwitterionic tryptophan in this conformation, characterized by the dihedral angles of the lateral chain $\chi_1 = -60$ and $\chi_2 = 100^\circ$ and the backbone dihedral angles $\Phi = -60$ and $\Psi = -90^\circ$.

To estimate the potential energy well that traps the tryptophan in this conformational state inside the membrane, a method of approximation was employed: keeping the molecular structure rigid, the residue was shifted through the interfaces along the *X*-direction and the potential energy was computed at each point. Accordingly, an energy barrier of around 16 kcal/mol confines this residue inside the membrane (Fig. 1b), however, due to the rounded potential shape, it stabilized inside the potential well oscillating with an amplitude of approximately 5 Å. The SMD simulations analyzed the system response while forcing the residue to surmount this energy barrier.

3.1.2. SMD simulations

3.1.2.1. General features of the system response due to the stiffness of the restraint. The kinetic, potential and total energy evolutions of the tryptophan SMD simulations with different springs are presented in Fig. 2a, c and e. A gradual increment of the potential energy until the residue exited the membrane (kinetic energy is kept relatively constant due to the thermal bath) and an energy step-like variation (identified by t_1 and t_2 arrows) were observed in all three simulations. This energy jump correlates to a χ_2-dihedral angle transition, from 100° to 150°, shown in Fig. 2b, d and f. The local average amplitude of the energy fluctuations estimated for k_3 (the stiffest spring) was $\Delta E \approx 0.6$ kcal/mol, being of the order of the thermal fluctuations at 300 K (i.e., $K_B T = 0.6$ kcal/mol, K_B = Boltzmann's constant and T = temperature). Since χ_2 conformational change was also observed in MD simulations (without restraint), this suggests that, even for the stiffest spring, no restrictions with respect to thermal fluctuations are being imposed by the spring force in the SMD simulations and that the effective barrier separating both states, in our model, should be of the order of the thermal energy. Accordingly, the calculated energy barrier for the χ_2-dihedral angle transition (from 100° to 150°) was around 1 kcal/mol.

Considering that the system is being sensed by an external oscillatory force of stiffness k, it is possible to estimate the displacement amplitudes (Δx) due to the thermal energy fluctuation, by means of the expression: $\Delta x = (K_B T/k)^{1/2}$ [2], and since $\delta_f = -k\Delta x$, then $\delta_f = -(K_B T k)^{1/2}$ (with $T = 300$ K). Therefore, for k_1, $\Delta x \approx 2.5$ Å and $\delta_f \approx 0.25$ kcal/mol Å; for k_2, $\Delta x \approx 1.0$ Å and $\delta_f \approx 0.60$ kcal/mol Å and for k_3, $\Delta x \approx 0.4$ Å and $\delta_f \approx 1.54$ kcal/mol Å. Data from simulations correspond well with these estimations. As a general rule, the average local amplitude of the force response is much smaller for a softer spring than for a stiffer one (compare Fig. 3a, c and e); the opposite occurs for the local amplitudes of the center of mass (compare Fig. 3b, d and f). Consequently, the χ_2 dihedral angle jumps (mentioned before) (signalized with t_1 and t_2 arrows in Fig. 3), were significantly more accentuated,

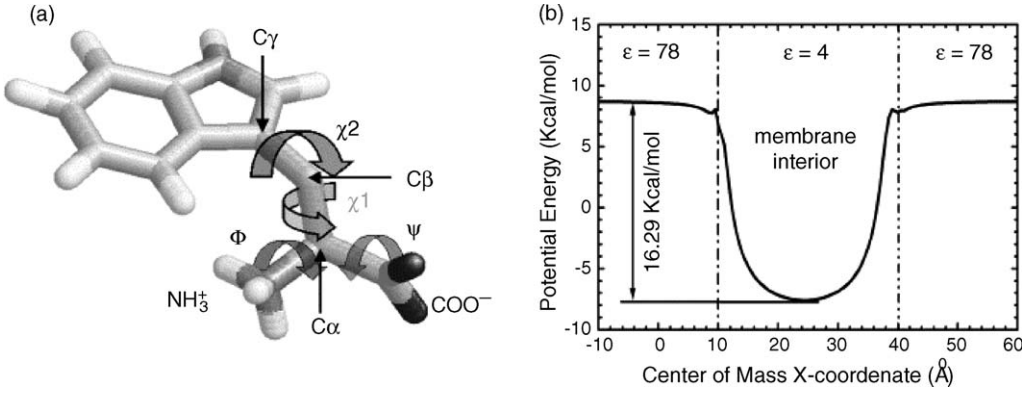

Fig. 1. (a) Cartoon representation of zwitterionic tryptophan amino acid with dihedral angles χ_1, χ_2, Φ and Ψ in the *perp*-$\chi_2(g^-)$ conformation. (b) Estimated potential energy profile for this conformation after 35 ns of molecular dynamics inside the membrane.

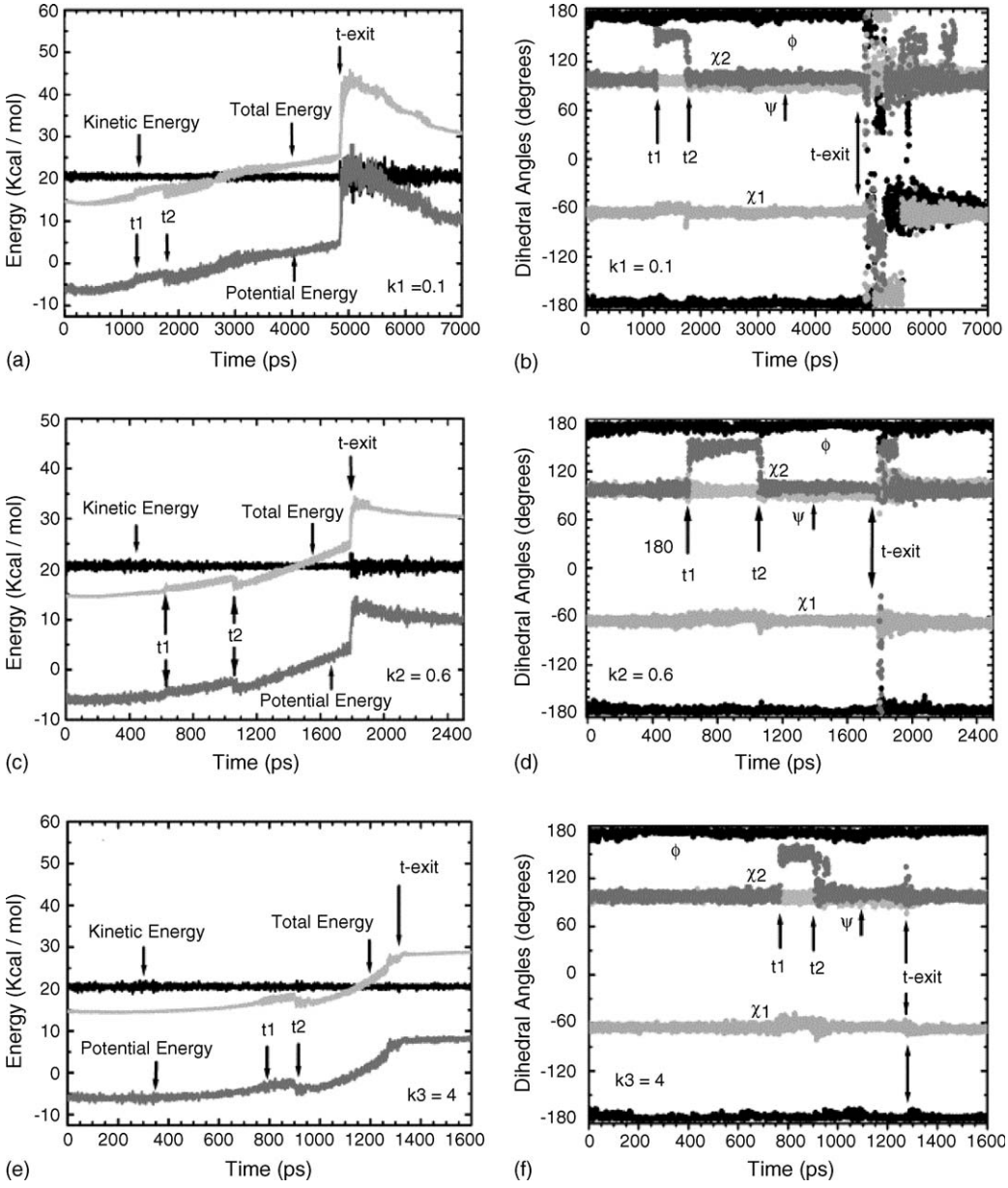

Fig. 2. Energies and conformational evolution of the SMD simulations performed with pulling velocity $V = 0.015$ Å/ps, C-terminal fixed to the spring and spring constant $k_1 = 0.1$ kcal/mol Å^2 in (a) and (b); $k_2 = 0.6$ kcal/mol Å^2 in (c) and (d) and $k_3 = 4$ kcal/mol Å^2 in (e) and (f). t_1 and t_2 arrows mark χ_2 dihedral angle jumps.

on the force profiles, when stiffer springs were considered (compare Fig. 3a, c and e).

From what it was exposed so far, in an overview of the system response, it can be predicted that softer springs will exert a less restricted action on the system and therefore, larger local displacements (Δx) and energy fluctuations (ΔE) will be expected. The consequence of this ''flexibility'' to explore the energy landscape is a force profile that will reflect global features [2] where the magnitude of some local events might be reduced or even vanished. Sensing the system response with different spring stiffness would provide different degrees of the details of the reaction force profile, which reflect how sensitive this detection methodology might be. It can be obtained a ''mean force profile'', as the one presented in Fig. 3a, where local events are vaguely reflected, or a ''detailed force profile'', as the one presented in Fig. 3c or e, where these local events are clearly exposed. However, if an extremely stiff spring is used, like k_3, exceedingly large amplitude fluctuations of the force profile might be observed, and some filtering must be considered in order to reveal the local events and the maximum force interaction value [1,6]. For example, Table 1 summarizes the statistical maximum interacting force obtained from several SMD simulations. Similar values were obtained with the three different spring constants, except for the extremely stiff spring k_3. In this case, Fig. 3e shows a wide variation of the interaction force at the exit time (±0.5 kcal/mol Å). Nevertheless, the statistical mean

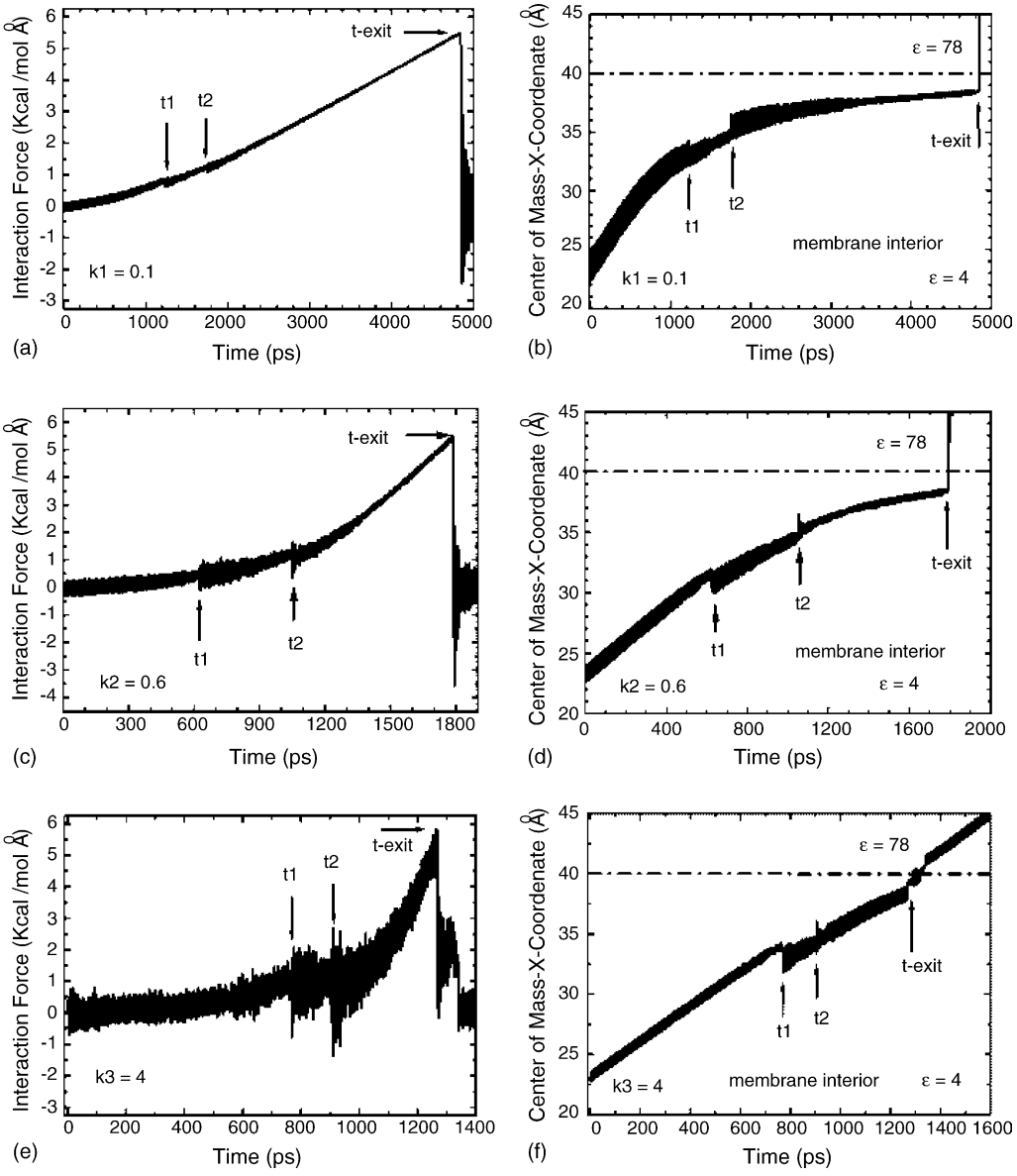

Fig. 3. Force profile as a function of time and center of mass trajectory in *X*-direction for the SMD simulations performed with pulling velocity $V = 0.015$ Å/ps, C-terminal fixed to spring and spring constant $k_1 = 0.1$ kcal/mol Å^2 in (a) and (b); $k_2 = 0.6$ kcal/mol Å^2 in (c) and (d) and $k_3 = 4$ kcal/mol Å^2 in (e) and (f). t_1 and t_2 arrows mark χ_2 dihedral angle jumps. The average local force amplitude increases with stiffens of the restraint, contrary to the average local amplitudes of the center of mass. For the stiffest spring (f), the residue is displaced at an almost constant velocity with an average value (0.013 Å/ps) quite similar to the pulling velocity (0.015 Å/ps).

Table 1
Maximum interaction force values and exit times for the SMD zwitterionic tryptophan simulations

Spring constant		Maximum interaction force		Time[a] (ps)
kcal/mol Å^2	pN/Å	kcal/mol Å	pN	
$k_1 = 0.1$	7	5.45 ± 0.07	379 ± 5	4716 ± 157
$k_2 = 0.6$	40	5.43 ± 0.08	377 ± 6	1683 ± 70
$k_3 = 4$	280	5.90 ± 0.06	410 ± 4	1177 ± 108

Statistical values over 10 simulations performed for each spring constant, with pulling velocity $V = 0.015$ Å/ps and C-terminal fixed to the spring.
[a] The exit times correspond to the maximum force.

force determined from 10 simulations performed with k_3 was 5.41 ± 0.07 kcal/mol Å, which is similar to the maximum force values obtained with softer springs. The maximum slope of the estimated potential profile of Fig. 1b, is 5 kcal/mol Å, this would give a rough estimation of the interaction force which is in good agreement with the values presented in Table 1.

To obtain the force response of a system, it is necessary to select the appropriate spring stiffness, which requires to explore a range of values from soft to stiff springs in order to adopt the one that better reveals the information hidden in the force profile. This is usually neither a soft nor an

extremely stiff spring. However, to reconstruct the potential of mean force some additional aspects must be considered.

3.1.2.2. Potential of mean force. According to M. Balsera and coworkers (1997), it is expected that the average applied force would measure the local slope of the energy potential, plus a frictional contribution that depends linearly on the pulling velocity only for a stiff spring [34]. However, in our classical dynamics approach and with an implicit medium model, the thermal bath merely accounts for the global effect of this medium, so no effective frictional coefficient is deduced from this type of representations (discussed in our previous work [21]). With this approach, in order to reconstruct the potential of mean force, the correlation of the force with the local slope of the energy profile can be directly determined from the SMD simulations without discounting the non-conservative energy due to local frictional effects. Fig. 4 illustrates this result.

Fig. 4a shows the force plotted against the displacement of the center of mass for the simulations performed with k_1 and k_3 spring constants. The estimated mean values for the force and for the position of the center of mass are locally quite similar for both curves because they are related to the potential energy slope at each point of the extraction pathway.

The reconstruction of the potential of mean force, illustrated in Fig. 4b, was obtained by plotting the potential energy versus the displacement, for the same two simulations mentioned above, where the step-like energy jump (interval t_1–t_2) corresponds to the χ_2-dihedral angle transition discussed before. The great similarity observed for both graphics of Fig. 4b with the potential well estimated by a static procedure (Fig. 1b), indicates that there is no dependence on any dynamic parameter (i.e. velocity or effective frictional coefficient) in this type of SMD simulations. In addition, the two opposite restraint stiffness (k_1 and k_3) were appropriate for reconstructing the energy landscape. A particular feature of the reconstructed potential profiles, shown in Fig. 4b, is the fewer amount of states that populates the top portion of the energy profile for the softer spring (k_1) curve, when compared to the stiffest spring (k_3) curve. This upper region of the energy landscape is characterized by a curvature change that, at a certain point (the exit point), it exceeded the k_1 spring stiffness, consequently, the system confinement was lost and the force profile showed a leap right after reaching its maximum value (shown in Fig. 4a). In addition, the locally unconfined energy fluctuations, shown in Fig. 2a and c for the softer springs, are represented by energy leaps right before the molecule leaves the membrane, i.e., at the top of the potential landscape. On the contrary, for the stiffest spring, the local energy fluctuations were confined along the entire simulation, and no energy gaps were observed (Fig. 2e). In this situation, many local states populated the upper part of the energy profile, as shown in Fig. 4b, facilitating the reconstruction of this region. A similar analysis was performed by E. Evans and K. Ritchie in a detailed theoretical work on energy landscape and bond strength for the case of receptor–ligand bond breakage [35]. The possibility of reproducing this type of results confirms the viability of applying SMD technique for studying membrane interacting molecules, even with a simple medium representation.

3.2. The AcWLKLL pentapeptide

3.2.1. MD simulations

This peptide was initially simulated in a homogeneous aqueous medium of dielectric constant $\varepsilon = 78$, and after 31 ns of dynamics the membrane was incorporated, leaving the system outside this medium, in the aqueous phase. The results of several MD simulations are summarized as follows:

No salt-bridge was formed in the polar medium (the distance criterion between the two center of charges was $d \leq 4$ Å for salt-bridge formation). The peptide adopted a stabilized conformation after 10–12 ns of dynamics. Fig. 5a shows this conformation after 31 ns of simulation in the aqueous medium where no salt-bridge was formed ($d = 7.7$ Å).

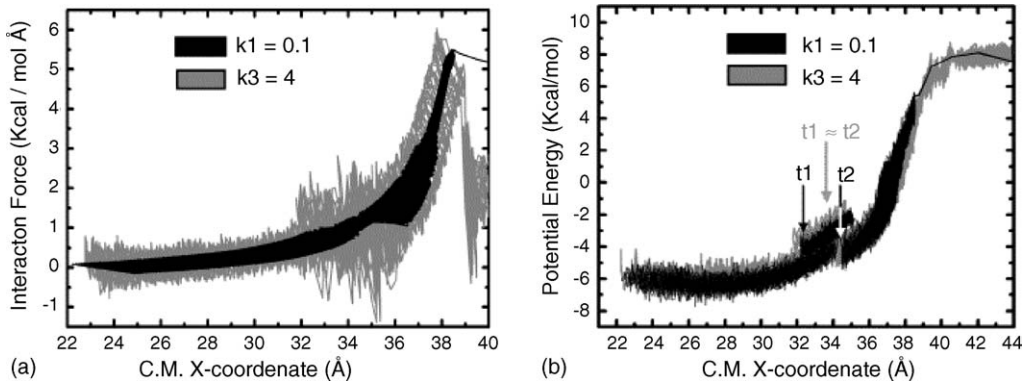

Fig. 4. Interaction force as a function of the center of mass displacement in *X*-direction in (a) and reconstruction of the potential of mean force in (b), for the simulations performed with $k_1 = 0.1$ and $k_3 = 4$ kcal/mol Å^2 spring constants. t_1 and t_2 arrows mark χ_2 dihedral angle jumps in (b).

The peptide spontaneously entered the membrane environment when simulated in the presence of this medium. Conformational changes in this medium induced the salt-bridge formation on the first 50 ps of dynamics. Fig. 5b shows the final conformation after 61 ns of simulation (d = 3.1 Å).

These results corroborate the experimental observations of Wimley and coworkers [16–18] indicating that the hydrophobic environment is essential to promote this type of interaction. More over, in resent simulations performed by M.P. Aliste with this pentapeptide in an explicit membrane representation [36], the salt-bridge formation was also exclusively observed inside the lipid bilayer and in the octanol phase. Comparing our results with Aliste's we also observed that: (a) Extended conformations were dominant in both polar and non-polar media (obtained by dynamic annealing method). (b) In water, the backbone dihedral angles were located in the β-region of the Ramachandran plot, however, inside the membrane, the backbone dihedral angles of the Leu-4 fall predominantly within the α-helix region. (c) The pentapeptide oriented parallel with respect to the interfaces. Aliste and coworkers also observed that this peptide located below the headgroups, in the lipid carbonyl region; however, in our case, it located at the center of the membrane. This disagreement might be due to the limitation of our model in describing the effect of the polar groups of the lipid heads and, in addition, we do not simulate two peptides simultaneously inside the membrane as in Aliste's work. (d) The ring of the tryptophan residue in the pentapeptide oriented almost perpendicular to the interfaces. (e) The salt-bridge began to form inside the membrane in the first picoseconds of dynamics and remained stable during the following 30 ns of simulation.

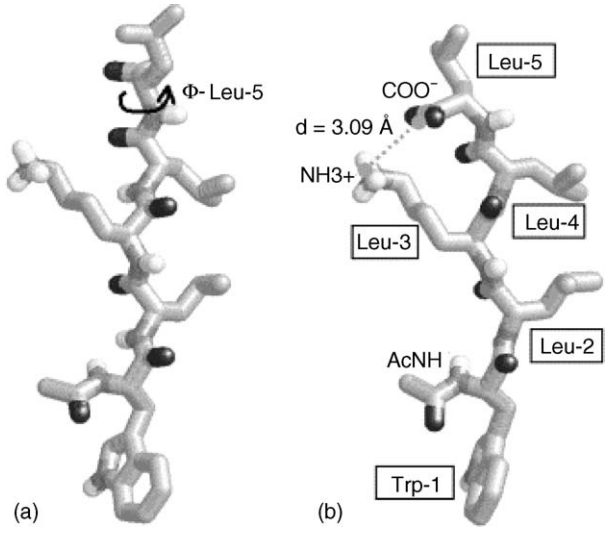

Fig. 5. AcWLKLL conformational sates and the corresponding estimated potential profiles. (a) Peptide cartoon representation after 31 ns of dynamics in aqueous medium of $\varepsilon = 78$ and (b) after insertion in the membrane environment, where the salt-bridge was formed (d = 3.09 Å). Figure (a) signalizes the 120° rotation of the Leucine-5 Φ dihedral angle, that allows the salt-bridge formation inside the membrane, as shown in (b). In (c) the corresponding estimated potential profiles for these two conformations are plotted. For the structure shown in (a), stabilized in the polar medium, a probable potential well of 3 kcal/mol (drawn in gray) would drive the peptide into the membrane. This potential profile would evolve into the second profile (in black) as the peptide gets into the membrane and forms the salt-bridge adopting the final conformation shown in (b).

3.2.2. SMD simulations

With the aim of analyzing the system response when varying the pulling-groups, the salt-bridge interaction was followed and the peptide–membrane interaction force as well as all conformational changes, were studied by means of SMD. Two SMD simulations are presented in this section. For the first simulation, the stabilized structure presented in Fig. 5b was considered as the initial state, and the peptide was pulled out of the membrane from the N-terminal region. In the second simulation, the peptide was pulled from the C-terminal, which is the region directly involved in the salt-bridge formation and a slightly different initial conformation was considered. To reveal the local events during the extraction pathway, a k_2 spring constant was considered in both cases.

The parameters for the two SMD simulations were the following:

- Pulling velocity V = 0.015 Å/ps (1.5 m/s)
- Spring constant k_2 = 0.6 kcal/mol Å (40 pN/Å)
- Pulling-group:
  (a) The carbon atom of the CH_3 group from the N-terminal
  (b) One of the oxygen atoms from the C-terminal (COO^-)

3.2.2.1. Simulation with the N-terminal fixed to the spring. Fig. 6 illustrates the center of mass trajectory along the X-direction and the force profile as a function of time, showing the correlation between the force response and the center of mass displacement along the simulation. Some significant events are marked with arrows, which are also shown in Fig. 7 illustrating the peptide position relative to the interface.

Fig. 6 shows that from the initial point at t = 0 ps to t_1 = 1291 ps, the force increases almost constantly, oscillating locally around a mean value. In this interval, the center of mass follows a similar pattern, and at t_1 is located at 5 Å of the membrane interface. Fig. 7 shows that the N-terminal has reached the interface at this time. From t_1 to t_2 = 1308 ps, Fig. 6 shows a drop of the force due to the displacement of the peptide towards the interface. During this t_1–t_2 interval, the N-terminal was extracted from the membrane and the system has also rotated along its axes; its new position is shown in Fig. 7. From t_2 to t_3 = 1491 ps, Fig. 6 shows a linear increment of the force without any peptide response (see also Fig. 7). The result of this force peak can be seen in Fig. 7 at t_4 = 1649 ps, being the extraction of great part of the

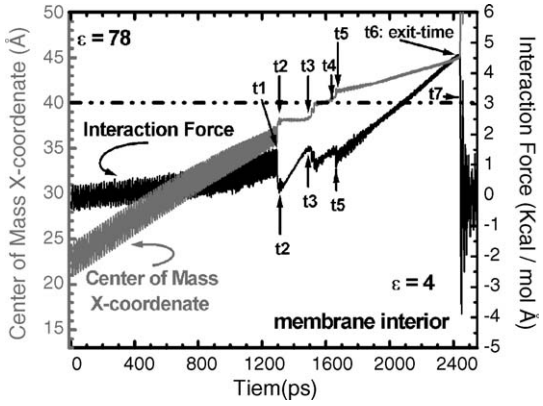

Fig. 6. Combined graphic of the interaction force and the center of mass evolution for the AcWLKLL SMD simulation performed with pulling velocity $V = 0.015$ Å/ps, N-terminal fixed to spring and spring constant $k_2 = 0.6$ kcal/mol Å^2. Seven moments, corresponding to significant events, were marked: $t_1 = 1291$ ps, $t_2 = 1208$ ps, $t_3 = 1491$ ps, $t_4 = 1649$ ps, $t_5 = 1664$ ps, $t_6 = 2436$ ps and $t_7 = 2445$ ps, with error bounds ± 0.5 ps determined from the simulation precision. t_6 corresponds to the exit-time and to the maximum interaction force value: 4.61 ± 0.01 kcal/mol Å (320.4 ± 0.7 pN).

peptide out of the membrane. In Fig. 6, it is observed that the center of mass has reached the interface at t_4, and that the next step forward, from t_4 to $t_5 = 1664$ ps, is again characterized by another staircase-type displacement of the center of mass and a small drop of the force. Consequently, another part of the peptide was extracted from the membrane during this interval (see Fig. 7). From t_5 to the exit time $t_6 = 2436$ ps, Fig. 6 shows that both, the center of mass and the interaction force, increase linearly in an average. Fig. 7 shows that during this period, the whole peptide translates while rotates in other to preserve the main interaction, i.e., the salt–bridge, inside the membrane. The last peak of the interaction force profile, which corresponds to its maximum value ($f_{max} = 4.61 \pm 0.01$ kcal/mol Å (320.4 ± 0.7 pN)), represents the extraction of this salt-bridge from the membrane, and consequently, the final breakage of the peptide–membrane interaction. No disruption of the salt-bridge was observed at the maximum force because the strength of this interaction, in the membrane environment, was much higher than the peptide-membrane interaction being sensed. However, after extracting the peptide, the salt-bridge was no longer stable in the aqueous medium. Statistical values obtained from 10 simulations where only different initial conditions were considered resulted in a maximum force of 4.60 ± 0.03 kcal/mol Å (320 ± 2 pN) and an exit time of 2117 ± 160 ps.

3.2.2.2. Simulation with the C-terminal fixed to the spring. Fig. 8 shows the center of mass trajectory along the *X*-direction and the force profile for the simulation performed with one of the C-terminal oxygen atoms fixed to the spring. Fig. 9 shows the peptide position relative to the interface.

Fig. 8 shows, an initial period, from $t = 0$ to $t_1 = 972$ ps, where the evolution presents similar characteristics as the previous simulation, a mainly translation towards the interface and an average increasing of the force. This simulation was initiated when the center of mass was located 7 Å closer to the interface in comparison with the previous simulation, so the exit-times are not directly comparable. Fig. 9 shows that the C-terminal of the peptide has reached the interface at t_1. From t_1 to $t_2 = 984$ ps, the force diminishes because the peptide has moved towards the interface (see Figs. 8 and 9). The center of mass is now located at the interface region. From t_2 to $t_3 = 1156$ ps, there is a linear increase of the force in the average with no variation of the center of mass location. The salt-bridge is still formed inside the membrane (see Fig. 9). At this point, Fig. 8 shows that the force has reached its maximum value ($f_{max} = 4.15 \pm 0.01$ kcal/mol Å (288.4 ± 0.7 pN)) and the result of this force peak is the extraction of the whole peptide out of the membrane environment; subsequently, the force decays drastically to zero (see Fig. 8). In this case, the peptide translation was almost parallel to the interface along the entire simulation without any significant rotation, because the external force was acting directly on the main interacting region. Statistical force and exit time values obtained from 10 simulations performed with slightly different initial conditions were 3.99 ± 0.08 kcal/mol Å (277 ± 6 pN) and 1303 ± 270 ps, respectively.

Figs. 6 and 8 presents two force profiles, representing the results of two sets of 10 simulations, performed with the N- and C-terminal as the pulling-groups. In addition, similar statistical maximum force values were determined for each set (4.60 ± 0.03 and 3.99 ± 0.08 kcal/mol Å). This result demonstrates the reproducibility of this method based on a simplified dynamic model. Furthermore, although quite different pathways have been followed, by pulling the peptide from different regions, the main interaction was equally revealed in both cases, which is the purpose of this type of steered dynamics. The observation that the salt-bridge was the main interaction for the molecule–membrane affinity process was in agreement with our analysis of the energy contribution of this interaction to the potential well (not shown).

Considering that interaction potentials are generally not known in advance, being able to recover this information by steered dynamics and to reveal the relative contributions of the interacting forces to the molecule–membrane affinity process is of great significance and can help to a better understanding of important biological responses.

3.2.2.3. Other results and conclusions. A summary of some general results obtained with this pentapeptide by combining the SMD parameters, is presented in Fig. 10. Each force profile of this figure, represents the results of a set of 10 simulations. Fig. 10a shows two profiles where the peptide was pulled from the N-terminal with the same pulling velocity $V = 0.015$ Å/ps. In the first place, the

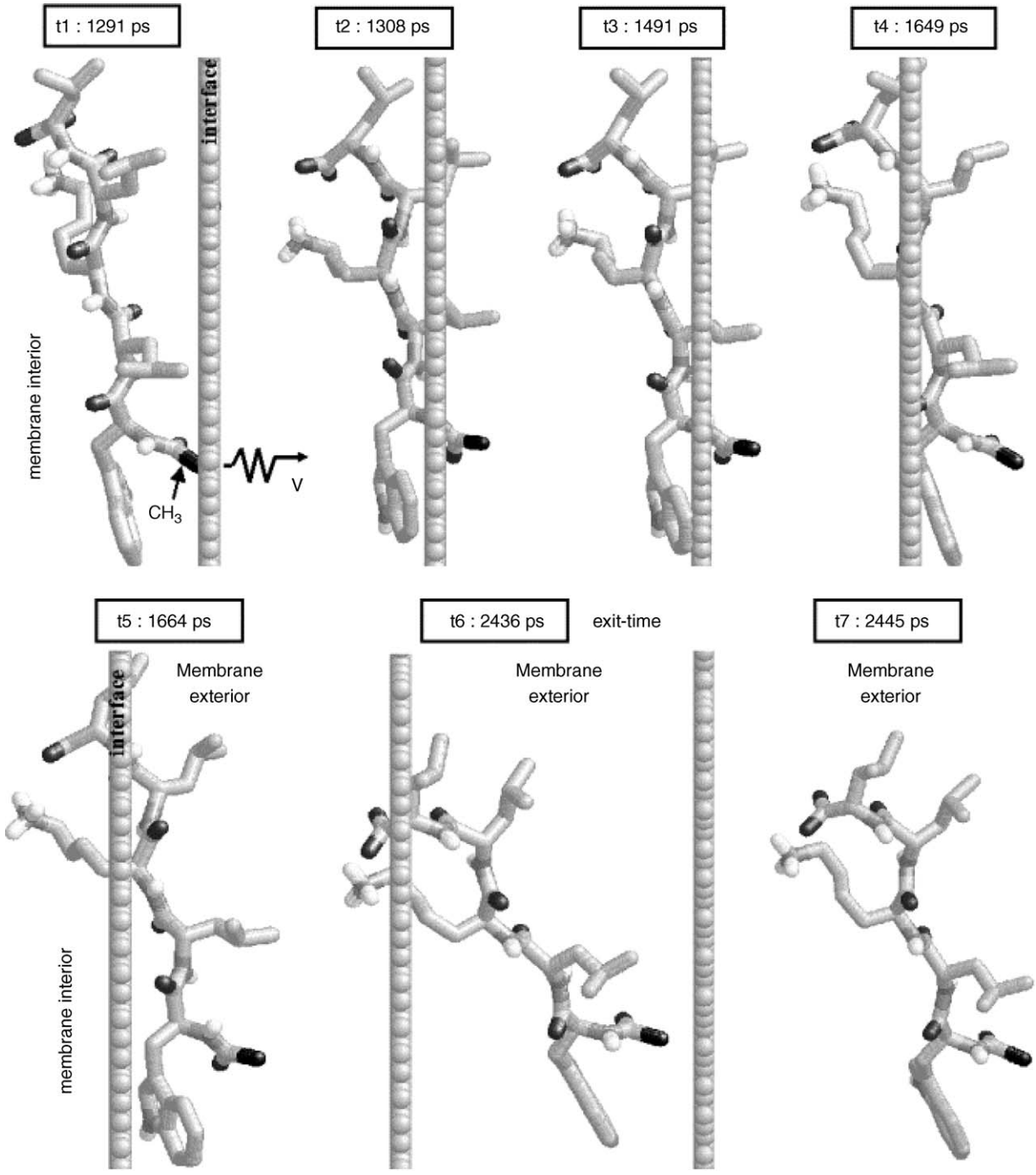

Fig. 7. Cartoon representation of the peptide positions relative to the membrane interface in the SMD simulation performed with pulling velocity $V = 0.015$ Å/ps, N-terminal fixed to spring and spring constant $k_2 = 0.6$ kcal/mol Å^2. All moments correspond with the presented in Fig. 6. The interface is schematically represented with no scaled proportions.

extraction was done with the softer spring of constants k_1 and, in the second place, with the stiff spring of constants k_2. These two cases are referred to N-V-k_1 and N-V-k_2, respectively. Fig. 10b shows two profiles where the peptide was pulled from the C-terminal with the spring constant k_2 and with pulling velocities V and $V_{1/2} = V/2$. These other two cases are referred to C-k_2-V and C-k_2-$V_{1/2}$, respectively. Accordingly, four representative force profiles are presented, obtained with the following parameters:

(a) Pulled-atom: carbon atom from CH_3 group (N-terminal), $V = 0.015$ Å/ps
   (1) $k_1 = 0.1$ kcal/mol Å^2 (referred to N-V-k_1 simulation)
   (2) $k_2 = 0.6$ kcal/mol Å^2 (referred to N-V-k_2 simulation)
(b) Pulled-atom: oxygen atom from COO^- group (C-terminal), $k_2 = 0.6$ kcal/mol Å^2
   (1) $V = 0.015$ Å/ps (referred to C-k_2-V simulation)
   (2) $V_{1/2} = 0.0075$ Å/ps ($V_{1/2} = V/2$) (referred to C-k_2-$V_{1/2}$ simulation)

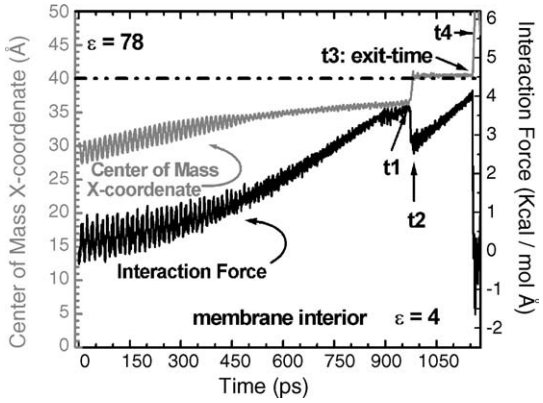

Fig. 8. Combined graphic of the interaction force and the center of mass evolution for the AcWLKLL SMD simulation performed with pulling velocity $V = 0.015$ Å/ps, C-terminal fixed to spring and spring constant $k_2 = 0.6$ kcal/mol Å^2. Four moments, corresponding to significant events, were marked: $t_1 = 972$ ps, $t_2 = 984$ ps, $t_3 = 1156$ ps, $t_4 = 1160$ ps, with error bounds ±0.5 ps determined from the simulation precision. t_3 corresponds to the exit-time and to the maximum interaction force value: 4.15 ± 0.01 kcal/mol Å (288.4 ± 0.7 pN).

Comparing the force profiles of simulations N-V-k_2 and N-V-k_1 from Fig. 10a, it is observed that: (a) The force profile shapes were conserved, therefore, same extraction pathways have been probably followed although different spring stiffness were used. (b) Softer springs lead to extended simulations. (c) In agreement with the tryptophan residue results, local effects reflected in the force profile are more attenuated for softer springs. (d) The statistical interaction force value for each case was quite similar: 5.29 ± 0.05 and 5.26 ± 0.03 kcal/mol Å, respectively. For the tryptophan simulations performed with different spring constants, the spontaneous χ_2 conformational change is observed in the force profiles. As a result of thermal fluctuations, this conformational fluctuation persisted for different periods, which leaded to different evolution pathways. However, similar interaction force values and potentials of mean force were also obtained from those simulations.

Comparing the force profiles of simulations C-k_2-V and C-k_2-$V_{1/2}$ from Fig. 10b, where only the pulling velocity was two-fold, it was confirmed that: (a) The extraction time in C-k_2-$V_{1/2}$ simulation was twice longer. (b) The force profile shape was also conserved and the statistical interaction force values obtained in these two cases were similar (3.99 ± 0.08 and 4.10 ± 0.05 kcal/mol Å, respectively).

Comparing the force profiles of simulations N-V-k_2 from Fig. 10a and C-k_2-V from Fig. 10b, where only different pulling-groups were considered, it was observed that force profile shapes were quite different as well as the statistical interacting force values (5.29 ± 0.05 vs. 3.99 ± 0.08 kcal/mol Å). The two groups of simulations have proceeded along different pathways and this may lead to different force interaction values.

To conclude, all previous observations for the pentapeptide can be summarized as follows: (1) Exit pathways and interaction force values were conserved when the pulling velocity or the spring constant were varied. (2) Different extraction pathways were followed when quite different conformations were compared (not shown), or when different pulling-groups were considered for the same conformations. The effect of selecting different pulling-groups on the system response has not been previously explored in other SMD simulations, although several studies were made with respect to the pulling velocity and the spring

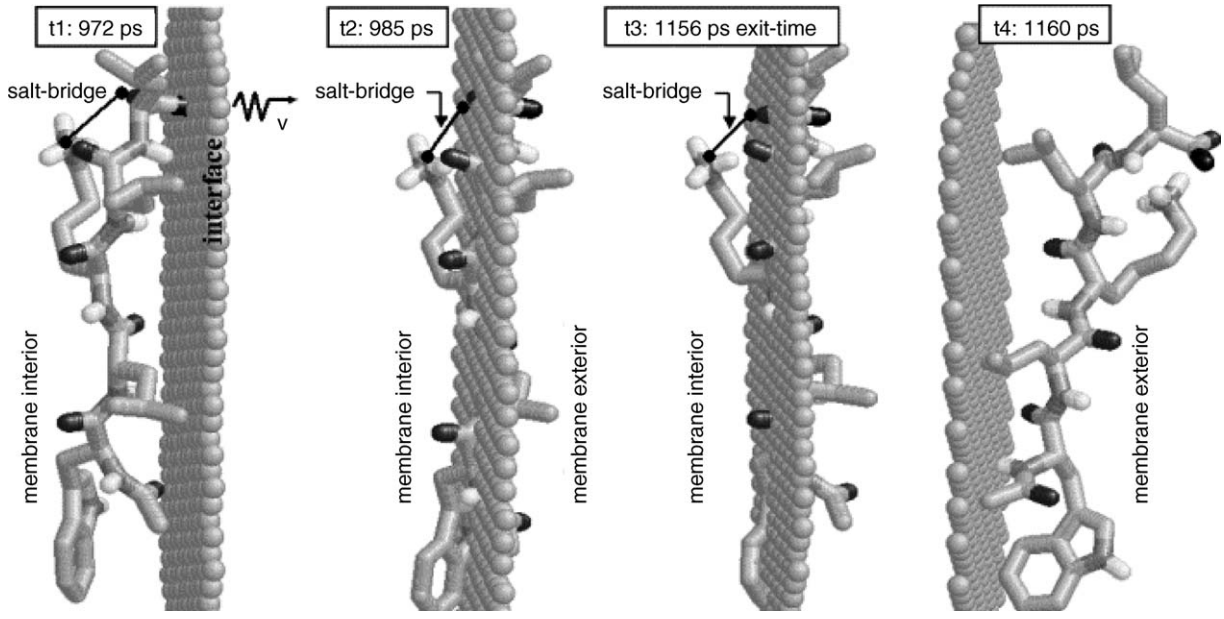

Fig. 9. Cartoon representation of the peptide positions relative to the membrane interface in the SMD simulation performed with pulling velocity $V = 0.015$ Å/ps, C-terminal fixed to spring and spring constant $k_2 = 0.6$ kcal/mol Å^2. All instants correspond with the presented in Fig. 8. The interface is schematically represented with no scaled proportions.

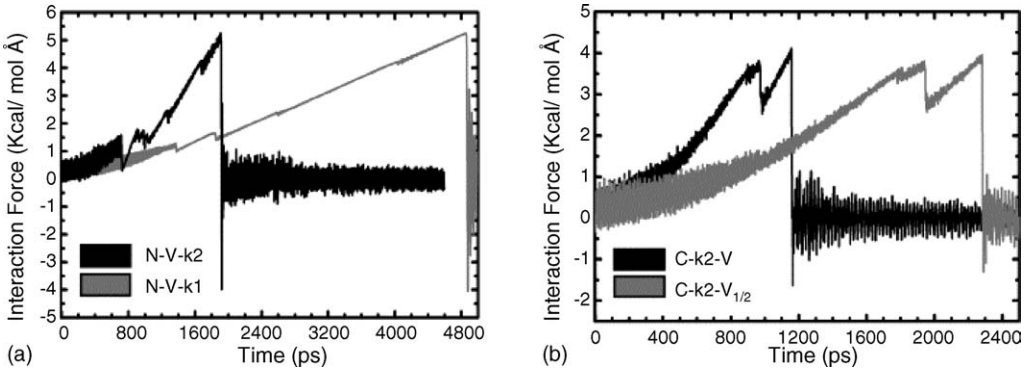

Fig. 10. Interaction force profiles of four AcWLKLL SMD simulations. In (a) both simulations were performed with the N-terminal fixed to the spring and $V = 0.015$ Å/ps, but two different spring constants $k_2 = 0.6$ kcal/mol Å^2 (stiff spring) for N-V-k_2 simulation and $k_1 = 0.1$ kcal/mol Å^2 (softer spring) for N-V-k_1 simulation. In (b) both simulations were performed with the C-terminal fixed to the spring and k_2, but two different pulling velocities V for C-k_2-V simulation and $V_{1/2} = 0.0075$ Å/ps = $V/2$ for C-k_2-$V_{1/2}$ simulation.

stiffness. Our simulations demonstrated that this parameter is quite important for determining the interaction pathway and consequently, diverse force responses.

Force profiles can reveal quite well different kind of molecular changes. Not only interaction forces and torsional angles transitions (conformational changes) but also displacements inside the membrane and rigid-body rotations will be reflected in these force profiles. This is mainly related to the anisotropic character of our membrane model, grounded in the induced polarization on both membrane surfaces, which depends on the location of the molecular charges relative to these interfaces. If an explicit membrane model were used, specific interactions, such as, the effect of the polar groups of the lipid heads on the charged regions of these molecules, will be added to the shapes of the characteristic force profiles.

For these reasons, the force profiles are like the ''fingerprints'' of the induced pathways and all events will be revealed in a hierarchical order according to their relevance in the biological problem that is being studied by SMD.

Small membrane interacting molecules and peptides are usually very flexible and do not present a defined conformation in the aqueous medium. They adopt stable conformations when exposed to the membrane environment where the degrees of freedom can be partially reduced due to the strengthening of the electrostatic interactions in the non-polar medium. For these molecules, the insertion pathways are highly variable. They follow extensive conformational changes while adapting to the membrane environment until a final stable conformational state is assumed. This behavior was seen and studied by means of MD and particularly, it provided information on the salt-bridge formation for the pentapetide, and on the overall conformational evolution of both systems. Consequently, for studying molecule–membrane interactions, steered dynamics needs to be implemented with a different purpose and approach. Taking advantage of the variability of the reaction pathways by exploring them, this methodology will reveal the relative contributions of various possible interactions and will expose the main forces that govern the molecular behavior in that medium. Therefore, for a molecule–membrane affinity problem, steered dynamics should look for those interactions that are, in a certain way, insensitive to the pulling parameters and that represent the driving forces for the interaction process.

With our simplified membrane model and by means of the SMD technique, we were able to reproduce several important results and observations reported by other investigators supporting the fact that most of them were inherent to the steered technique and that they can also be recovered in a molecule–membrane interaction study. If an explicit membrane representation were used, a further detailed exploration of the system response can be expected, where specific solute-membrane and solvent–solute interactions might also be exposed and will contribute to the fingerprints of the characteristic potential profiles. Even so, we can still rely on our observations and adopt the appropriate combination of the SMD parameters to perform a precise analysis of any biological system.

Acknowledgments

This work was supported by a doctoral fellowship granted by CNPq, Brazil.

References

[1] H. Grubmüller, B. Heymann, P. Tavan, Ligand binding: molecular mechanics calculation of streptavidin–biotin rupture force, Science 271 (1996) 997–999.
[2] S. Izrailev, S. Stepaniants, M. Balsera, Y. Oono, K. Schulten, Molecular dynamics of unbinding of the avidin–biotin complex, Biophys. J. 72 (1997) 1568–1581.
[3] B. Isralewitz, M. Gao, K. Schulten, Steered molecular dynamics and mechanical functions of proteins, Curr. Opin. Struct. Biol. 11 (2001) 224–230.
[4] S-J. Marrink, O. Berger, P. Tieleman, F. Jähnig, Adhesion forces of lipids in a phospholipid membrane studied by molecular dynamics simulations, Biophys. J. 74 (1998) 931–943.

[5] S. Izrailev, A.R. Crofts, E.A. Berry, K. Schulten, Steered molecular dynamics simulation of the rieske subunit motion in the cytochrome bc1 complex, Biophys. J. 77 (1999) 1753–1768.
[6] B. Heymann, H. Grubmüller, ANO2/DNP-happen unbinding forces studied by molecular dynamics atomic force microscopy simulations, Chem. Phys. Lett. 303 (1999) 1–9.
[7] H. Lu, B. Isralewitz, A. Krammer, V. Vogel, K. Schulten, Unfolding of titin immunoglobulin domains by steered molecular dynamics simulation, Biophys. J. 75 (1998) 662–671.
[8] M.V. Bayas, K. Schulten, D. Leckband, Forced detachment of the CD2-CD58 complex, Biophys. J. 84 (2003) 2223–2233.
[9] A.C. Lorenzo, E.R. Caffarena, Elastic properties-Young's modulus determination and structural stability of the tropocollagen molecule: a computational study by Steered Molecular Dynamics, J. Biomech. 65/7 (2005) 1527–1533.
[10] H. Jäckle, P.L. Luisi, Conformational study of histidine- and tryptophan-containing peptides in solution based upon the combination of nuclear magnetic resonance, circular dichroism, and fluorescence measurements, J. Phys. Chem. 88 (1984) 1767–1777.
[11] J.B.A. Ross, H.R. Wyssbroard, R.A. Poter, G.P. Schwartz, C.A. Michaels, W.R. Laws, Correlations of tryptophan fluorescence intensity decay parameters with ^{1}H NMR-determined rotamers conformations: [tryptophan^{2}] oxytocin, Biochemistry 31 (1992) 1585–1594.
[12] J.W. Ponder, F.M. Richards, Tertiary templates for proteins. Use of packing criteria in the enumeration of allowed sequences for different structural classes, J. Med. Biol. 193 (1987) 775–791.
[13] R.A. Engh, L.X.Q. Chen, G.R. Fleming, Conformational dynamics of tryptophan: a proposal for the origin of the non-exponential florescence decay, Chem. Phys. Lett. 126 (3/4) (1986) 365–372.
[14] H.L. Gordon, H.C. Jarrell, A.G. Szabo, K.J. Willis, R.L. Somorjai, Molecular dynamics simulations of the conformational dynamics of tryptophan, J. Phys. Chem. 96 (4) (1992) 1915–1921.
[15] P.G. Pascutti, E.P.G. Areas, A.S. Ito, K.C. Mundin, P.M. Bisch, Molecular dynamics of peptides at membrane-water interfaces, Progress Biophys. Mol. Biol. 65 (Suppl. 1) (1996) 49.
[16] W.C. Wimley, K. Gawrisch, T.P. Creamer, S.H. White, Direct measurements of salt-bridge energies using a peptide model system: Implications for protein stability, Proc. Natl. Acad. 93 (1996) 2985–2990.
[17] W.C. Wimley, T.P. Creamer, S.H. White, Solvation energies of amino acid side chains and backbone in a family of host–guest pentapeptides, Biochemistry 35 (1996) 5109–5124.
[18] W.C. Wimley, S.H. White, Experimentally determined hydrophobicity scale for proteins at membrane interfaces, Nat. Struct. Biol. 3 (1996) 842–848.
[19] E.P.G. Arêas, P.G. Pascutti, S. Schreier, K.C. Mundim, P.M. Bisch, Molecular dynamics simulations of signal sequence at a membrane/water interface, J. Phys. Chem. 99 (1995) 14882.
[20] P.G. Pascutti, K.C. Mundim, A.S. Ito, P.M. Bisch, Polarization effects on peptide conformations at water–membrane interface by molecular dynamics simulation, J. Comp. Chem. 20 (9) (1999) 971–982.
[21] A.C. Lorenzo, P.G. Pascutti, P.M. Bisch, Non-specific interaction forces at water–membrane interface by forced molecular dynamics simulations, J. Comp. Chem. 24 (2003) 328–339.
[22] W.F. van Gunsteren, H.J.C. Berendsen, Groningen Molecular Simulation (GROMOS) Library Manual, Biomos, Groningen, 1987.
[23] W.R.P. Scott, P.H. Hunenberger, I.G. Tironi, A.E. Mark, S.R. Billeter, J. Fennen, A.E. Torda, T. Huber, P. Kruger, W.F. van Gunsteren, et al. The GROMOS biomolecular simulation program package, J. Phys. Chem. 103 (1999) 3596–3607.
[24] J.N. Israelachvilli, Intermolecular and Surface Forces, 2nd ed., Academic Press, 1991.
[25] M. Uematsu, E.U. Franck, J. Phys. Chem. 9 (1980) 1291–1306.
[26] C. Tandford, The Hydrophobic Effect, Wiley, New York, 1973/1980.
[27] J.R. Reizt, F.J. Milford, R.W. Christy, Foundations of Electromagnetic Theory, Addison-Wesley, Reading, MA, 1967.
[28] J.D. Jackson, Classical Electrodynamics, Wiley, New York, 1962.
[29] P.G. Pascutti, M.M. Cassiano, A.S. Ito, K.C. Mundin, P.M. Bisch, Molecular dynamics simulations of peptides–membrane interactions, Biophys. J. 72 (2) (1997) 196.
[30] P.G. Pascutti, L.J. El-Jaik, K.C. Mundim, A.S. Ito, P.M. Bisch, Molecular dynamics simulation of α-melanocyte stimulating hormone in a water–membrane model interface, Eur. Biophys. J. 28 (1999) 499–509.
[31] F.S. Leite, P.G. Pascutti, C.B. Anteneodo, Molecular modeling and dynamics of the sodium channel inactivation gate, Biophys. J. 82 (3) (2002) 1207–1215.
[32] K.B. Wiberg, A scheme for strain energy minimization. Application to the cycloalkanes, J. Am. Chem. Soc. 87 (5) (1965) 1070–1078.
[33] H.J.C. Berendsen, J.P.M. Postma, W.F. van Gunstern, A. DiNola, J.R. Haak, Molecular dynamics with coupling to an external bath, J. Chem. Phys. 81 (1984) 3684–3690.
[34] M. Balsera, S. Stepaniants, S. Izrailev, Y. Oono, K. Schulten, Reconstructing potential energy functions from simulated force-induced unbinding processes, Biophys. J. 73 (1997) 1281–1287.
[35] E. Evans, K. Ritchie, Dynamic strength of molecular adhesion bonds, Biophys. J. 72 (1997) 1541–1555.
[36] M.P. Aliste, J.L. MacCallum, D.P. Tieleman, Molecular dynamics simulations of pentapeptides at interfaces: salt bridge and cation–π interactions, Biochemistry 42 (2003) 8976–8987.